Theory of interactions of surface-optical phonons with surface space-charge waves in doped GaAs

B. G. Martin
Analysis Consultants, El Toro, California 92630

R. F. Wallis
Institute for Surface and Interface Science and Department of Physics, University of California, Irvine, Irvine, California 92717

(Received 21 February 1989)

A theoretical investigation has been made of the interaction of surface-optical phonons and surface space-charge waves (SSCW's) in a solid-state plasma, namely, doped GaAs. In obtaining the dispersion relation, the specular-reflection approach of Kliewer and Fuchs [Phys. Rev. **172**, 608 (1968)] was used. Dispersion curves have been obtained both neglecting and taking into account carrier damping. The results indicate that amplification of the slow SSCW occurs for a frequency range beginning at the transverse-optical-phonon frequency and ending at the surface-optical-phonon frequency. There are corresponding threshold and termination wave vectors. Since slow SSCW's are negative-energy waves, they can lead to an amplifying instability by coupling to a positive-energy optical phonon.

I. INTRODUCTION

Surface electromagnetic-wave instabilities in doped semiconductors have been the subject of many theoretical and experimental investigations over the last two decades or so (see the representative references 1–14, and citations therein). Of interest in the present paper are surface space-charge wave instabilities associated with their interaction with optical phonons.[15–18] This subject was considered previously by Tajima and Ushioda,[15] who obtained the dispersion relation by assuming an isotropic dielectric tensor and ignoring off-diagonal elements. In addition, carrier damping was not taken into account.

Tajima and Ushioda reported that varying the plasma frequency, which is proportional to the square root of the carrier concentration, has an effect on the electromagnetic-wave–phonon interactions. Specifically they found that for $\omega_p < \omega_T$, where ω_p is the plasma frequency and ω_T the transverse-optical-phonon frequency, there is an amplifying instability, while for $\omega_p > \omega_T$, there is none. The latter result differs from that reported in the present paper.

In what follows, we obtain the surface-electromagnetic-wave dispersion relation for polar semiconductors including retardation and the presence of a dc current. The spectacular-reflection boundary condition of Kliewer and Fuchs[19] is used. Numerical results are then presented for doped GaAs, both with and without carrier damping taken into account. In addition, the results of an analysis of the dispersion instabilities obtained are discussed. A comparison is made with previously published results, and conclusions are presented.

II. THEORY

Consider a semiconductor which is infinite in the x and y directions, semi-infinite in the z direction, and characterized by a wave-vector- and frequency-dependent dielectric tensor $\epsilon_{\alpha\beta}(\mathbf{k},\omega)$ when a dc current associated with the drift velocity $\mathbf{V}_0$ of the charge carriers is present. The other half-space is filled by a dielectric with dielectric constant ϵ_d. In what follows, we use the nonlocal Maxwell equations for this geometry to obtain expressions relating the field and dielectric-tensor components. The specular-reflection technique of Kliewer and Fuchs is used to obtain the dispersion relation.

To obtain $\epsilon_{\alpha\beta}$, we proceed by linearizing the transport equation for the motion of an average carrier in the semiconductor. The nonlocal conductivity tensor thus obtained is[12]

$$\sigma_{\alpha\beta}(\mathbf{k},\omega)=N_0 q\left[M_{\alpha\beta}(\mathbf{k},\omega)+\frac{V_{0\alpha}}{\omega-\mathbf{k}\cdot\mathbf{V}_0}\sum_\gamma k_\gamma M_{\gamma\beta}(\mathbf{k},\omega)\right], \tag{2.1}$$

where N_0 is the equilibrium carrier density, q is the charge of a carrier, $\mathbf{V}_0$ is the drift velocity, and the matrix $\overleftrightarrow{\mathbf{M}}$ is given by

$$\overleftrightarrow{\mathbf{M}}=\frac{iq}{a}\begin{bmatrix}\omega-(K_y V_{0y}+k_z V_{0z}) & k_x V_{0y} & k_x V_{0z}\\ k_y V_{0x} & \omega-(k_x V_{0x}+k_z V_{0z}) & k_y V_{0z}\\ k_z V_{0x} & k_z V_{0y} & \omega-(k_x V_{0x}+k_y V_{0y})\end{bmatrix}. \tag{2.2}$$

The quantity a is given by $a=m^*\omega(\omega-\mathbf{k}\cdot\mathbf{V}_0+i\nu)$, where m^* is the carrier effective mass and ν is the carrier damping frequency. The components of the dielectric tensor are given by

$$\epsilon_{\alpha\beta}(\mathbf{k},\omega)=\delta_{\alpha\beta}\epsilon_\infty+\frac{4\pi i}{\omega}\sigma_{\alpha\beta}(\mathbf{k},\omega)\ , \tag{2.3}$$

where $\delta_{\alpha\beta}$ is the Kronecker delta and ϵ_∞ is the high-frequency dielectric constant of the semiconductor.

The dielectric tensor specified by Eqs. (2.1)–(2.3) is for the case of a dc current interacting with surface polaritons in a nonpolar semiconductor.[9] We now consider the case of a polar semiconductor, where the interaction with optical phonons must be taken into account. This is quite easy as far as components of the dielectric tensor are concerned: one merely needs to add the term $\epsilon_\infty(\omega_L^2-\omega_T^2)/(\omega_T^2-\omega^2)$ to the diagonal elements. In this expression ω_L is the longitudinal-optical-phonon frequency and ω_T is the transverse-optical-phonon frequency.

In seeking solutions to the Maxwell equations, it is assumed that the electromagnetic waves propagate in the y direction and that the Cartesian components of the electric field $\mathbf{E}$ have the form

$$\mathbf{E}(\mathbf{r},t)=(0,\mathbf{E}_y(z),\mathbf{E}_z(z))\exp[i(k_y y-\omega t)]\ , \tag{2.4}$$

where k_y is the wave-vector component in the direction of propagation, and ω is the frequency. The drift velocity $\mathbf{V}_0$ is also taken in the y direction: $\mathbf{V}_0=(0,V_0,0)$. Only p polarization is considered, i.e., the situation where the electric vector lies in the sagittal plane defined by the direction of propagation, and the normal to the surface. For this configuration, the field variables do not depend on x, and the wave vector $\mathbf{k}$ in $\epsilon_{\alpha\beta}(\mathbf{k},\omega)$ can be taken to be $\mathbf{k}=(0,k_y,k_z)$.

Following the Kliewer-Fuchs specular-reflection approach, we have derived the surface polariton dispersion relation, which can be expressed as

$$1+\frac{\omega^2\epsilon_d}{\pi c^2\alpha_0}\int_{-\infty}^{\infty}dk_z\,\frac{T_{zz}}{T_{zz}T_{yy}-T_{yz}^2}=0\ , \tag{2.5}$$

where α_0 is the decay coefficient for the dielectric given by

$$\alpha_0^2=k_y^2-\epsilon_d\frac{\omega^2}{c^2}\ , \tag{2.6}$$

and the quantities in the integrand of Eq. (2.2) are given by

$$T_{yy}=\frac{\omega^2}{c^2}\epsilon_{yy}(\mathbf{k},\omega)-k_z^2\ , \tag{2.7}$$

$$T_{zz}=\frac{\omega^2}{c^2}\epsilon_{zz}(\mathbf{k},\omega)-k_y^2\ , \tag{2.8}$$

$$T_{yz}=T_{zy}=\frac{\omega^2}{c^2}\epsilon_{yz}(\mathbf{k},\omega)+k_y k_z\ . \tag{2.9}$$

Using the above tensor elements and Eq. (2.2), one obtains the dispersion relation

$$\frac{\epsilon_\infty}{\epsilon_d}\left|\epsilon_p-\frac{\omega_p^2}{(\omega-k_yV_0)(\omega-k_yV_0+i\nu)}\right|\left|1-\frac{\epsilon_\infty\epsilon_p\omega_p^2V_0^2/c^2}{\omega_p^2-\epsilon_p(\omega-k_yV_0)(\omega-k_yV_0+i\nu)}\right|^{1/2}=-\frac{\alpha}{\alpha_0}\ , \tag{2.10}$$

where α is the decay constant for the semiconductor specified by

$$\alpha^2=k_y^2-\frac{\epsilon_\infty\omega^2}{c^2}\left[\epsilon_p-\frac{\omega_p^2}{\omega^2}\frac{\omega-k_yV_0}{\omega-k_yV_0+i\nu}\right]\ , \tag{2.11}$$

$$\epsilon_p=\left[\frac{\omega_l^2-\omega^2}{\omega_T^2-\omega^2}\right]\ , \tag{2.12}$$

$$\omega_p^2=\frac{4\pi N_0q^2}{\epsilon_\infty m^*}\ . \tag{2.13}$$

It is of interest to investigate the dispersion relation for the nonretarded limit (i.e., $c\to\infty$):

$$\frac{\epsilon_\infty}{\epsilon_d}\left[\epsilon_p-\frac{\omega_p^2}{(\omega-k_yV_0)(\omega-k_yV_0+i\nu)}\right]=-1\ . \tag{2.14}$$

Neglecting damping and solving for the wave vector k_y, one obtains the result

$$k_y=\frac{\omega}{V_0}\pm\frac{\omega_p}{V_0}\left[\frac{\epsilon_\infty(\omega_T^2-\omega^2)}{\omega_T^2+\epsilon_\infty\omega_L^2-\omega^2(1+\epsilon_\infty)}\right]^{1/2}\ , \tag{2.15}$$

where has been taken to equal unity corresponding to vacuum. For frequencies in the range

$$\omega_T^2<\omega^2<\frac{\omega_T^2+\epsilon_\infty\omega_L^2}{1+\epsilon_\infty}\equiv\omega_{SO}^2\ , \tag{2.16}$$

the expression under the radical in Eq. (2.15) is negative and hence k_y consists of complex-conjugate pairs. For the + sign we have an exponentially decaying wave in the direction of propagation, while for the − sign, we have an exponentially amplified wave. Note from Eq. (2.15) that the gain for the amplified wave increases with increasing plasma frequency ω_p, i.e., with increasing carrier concentration. When the frequency ω lies outside the range given by Eq. (2.16), there are no amplifying or decaying waves. Equation (2.16) essentially defines the threshold and cutoff frequencies, the latter being the limiting surface-optical-phonon frequency for large wave vector, ω_{SO}, defined as the positive square root of the fraction in Eq. (2.16). There are also threshold and cutoff wave vectors, which can be obtained from Eq. (2.15) by looking at frequencies where $dk_y/d\omega=0$.

In the absence of optical phonons, Eq. (2.15) reduces to

$$k_y=\frac{\omega}{V_0}\pm\frac{\omega_p}{V_0}\left[\frac{\epsilon_\infty}{1+\epsilon_\infty}\right]^{1/2}\ , \tag{2.17}$$

the dispersion relation for surface space-charge waves

(SSCW's). Here the wave vector is real; hence, it is the presence of optical phonons that gives rise to amplifying instabilities for the geometry under consideration here. The slow and fast SSCW's can be thought of as, respectively, negative-energy waves ($\omega < kV_0$) and positive-energy waves ($\omega > kV_0$). A negative-energy wave can cause an instability by coupling to a positive-energy wave, e.g., an optical phonon as in Eq. (2.15), as well as to a dissipative medium, e.g., the resistive wall of Birdsall *et al.*[20]

Taking the limit $V_0=0$ in the dispersion relations gives the coupled surface-plasmon–surface-optical-phonon modes. For example, in the nonretarded case, Eq. (2.14), the coupled-mode dispersion relation is

$$\epsilon_\infty \frac{\omega_L^2-\omega^2}{\omega_T^2-\omega^2} - \frac{\epsilon_\infty \omega_p^2}{\omega^2} = -1 \ . \tag{2.18}$$

III. RESULTS AND DISCUSSION

The theoretical dispersion curves have been obtained for surface waves in GaAs in the presence of drifting current carriers. Some of the results include the effects of retardation, as well as the effect of damping resulting from the scattering of carriers. Optical-phonon damping is neglected here because it is generally small compared with carrier damping. In the first set of calculations, the frequency ω was taken as real and the dispersion relation was solved for complex wave vector $k_y = k_1 \pm ik_2$.

For GaAs, at 300 K, $\epsilon_0 = 12.85$ and $\epsilon_\infty = 10.88$.[5] The Lyddane-Sachs-Teller relation is

$$\frac{\epsilon_0}{\epsilon_\infty} = \frac{\omega_L^2}{\omega_T^2} \ , \tag{3.1}$$

so that we have

$$\frac{\omega_L}{\omega_T} = 1.09 \ . \tag{3.2}$$

A. Nonretarded limit

For the nonretarded limit, the dispersion relation, neglecting carrier damping, is given by Eq. (2.15). This equation was used to obtain the dispersion results shown in Fig. 1.

For frequencies $\omega < \omega_p$ there are two SSCW branches labeled *a* and *b*, where *a* corresponds to the fast SSCW and *b* to the slow SSCW. At $\omega = \omega_T$, the two branches merge to form the doubly degenerate branch *ab* having a complex-conjugate pair of wave vectors, one of which corresponds to an amplifying slow SSCW–optical-phonon instability. The other complex-conjugate wave vector corresponds to a decaying wave. At $\omega = \omega_{SO}$, branch *ab* terminates, and we recover the two SSCW branches *a* and *b*. This is similar to behavior noted before in the absence of optical phonons,[14] where a semiconductor with drifting carriers is placed next to a semiconductor having zero drift velocity, and is described by a Drude dielectric function. For this case, the nondrifted plasma wave associated with the Drude dielectric function plays a role analogous to that of the optical phonons. For frequencies beyond the instability termination point, ω_{SO}, the *a* and *b* branches approach one another and then become parallel as shown in Fig. 1.

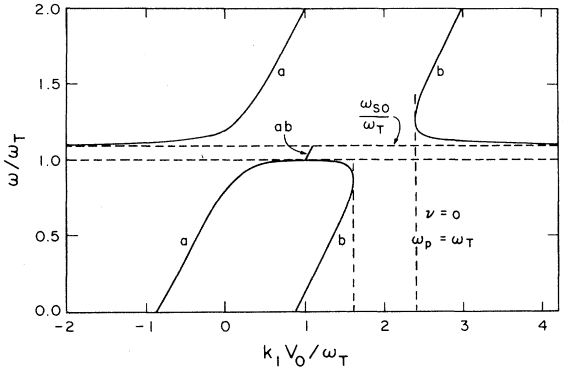

FIG. 1. Dispersion curves in the nonretarded limit without damping for $\omega_p = \omega_T$.

The vertical dashed lines in Fig. 1 indicate the range of reduced wave vector encompassing the convect.. ·stability. This in turn defines the threshold and termination drift velocities for amplification.

The frequency dependence of the imaginary part of each wave vector for branch *ab* is of interest. The gain (or decay) increases with increasing frequency from $\omega = \omega_T$, until it reaches a maximum and then abruptly drops to zero at $\omega = \omega_{SO}$. In fact just below ω_{SO}, the gain becomes infinite, but only because carrier damping has been neglected.

B. Retardation effects neglecting carrier damping

Next we consider the dispersion relation including retardation [Eq. (2.10)]. This equation is of fourth degree in wave vector, and thus there are four branches rather than the two obtained in the nonretarded limit. The results were obtained numerically using real values of frequency as input and calculating values of wave vector. In these calculations, $V_0/c = 0.001$. Figures 2 and 3 show dispersion curves for negative and positive values of wave

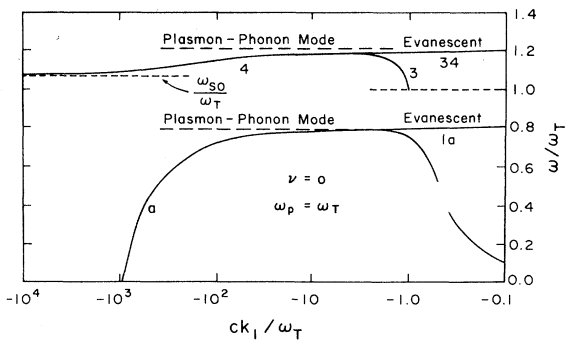

FIG. 2. Retarded dispersion curves without damping for $\omega_p = \omega_T$ and negative wave vector.

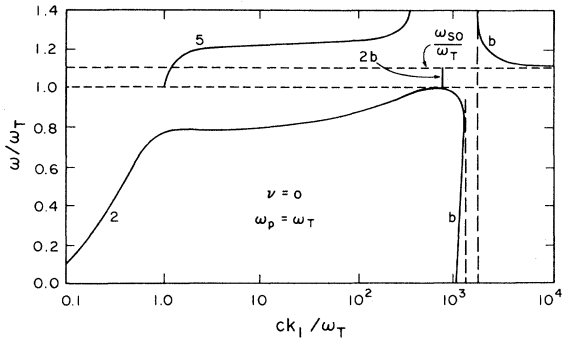

FIG. 3. Retarded dispersion curves without damping for $\omega_p=\omega_T$ and positive wave vector.

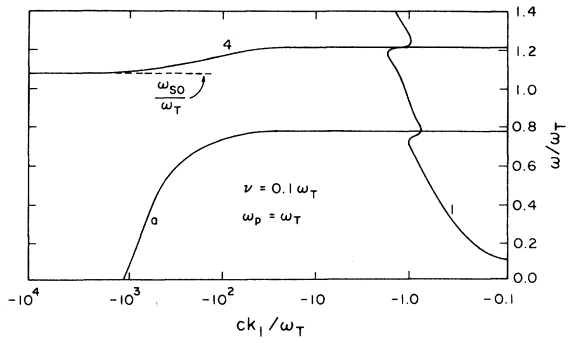

FIG. 4. Retarded dispersion curves with damping for $\omega_p=\omega_T$ and negative wave vector.

vectors, respectively. As before we have taken $\omega_p=\omega_T$. Note that, compared with Fig. 1, the form of the reduced wave vector has been changed from $k_y V_0/\omega_T$ to ck_y/ω_T.

For frequencies $\omega<\omega_T$, we have the SSCW branches *a* and *b* as in the nonretarded case. In addition, we have the polariton branches 1 and 2, which result from taking into account retardation. For negative wave vectors (Fig. 2), one sees that as ω increases, branch 1, a polariton mode, couples with branch *a*, the fast SCW mode, to give the degenerate branch 1*a*, an evanescent wave which terminates at $k_1=0$. Further investigation of this branch shows that for very small values of k_1, the branch bends upward and terminates asymptotically at $k_1=0$, at which point the decay constant α_0 is pure imaginary, and we no longer have a surface mode. However, the inclusion of carrier damping restores the surface modes (the decay constant is no longer pure imaginary at $k_1=0$). The effect of damping is discussed in the next section (III C). This type of behavior also occurs in the absence of phonons.[14] When $\omega=\omega_T$, another polariton mode, branch 3, begins and moves to the left with increasing frequency. For $\omega\geq\omega_{SO}$, a phononlike mode, branch 4, moves in toward branch 3. They couple, forming another evanescent branch, 34, that behaves similarly to branch 1*a* discussed above. In addition, the coupled plasmon-phonon modes in the absence of a dc current are indicated.

Consider next Fig. 3, the situation for positive wave vectors. For $\omega\leq 0.8\omega_p$, branch 2 is polaritonlike, but becomes phononlike as ω approaches ω_T. At ω_T, branches 2 and *b* come together to form degenerate branch 2*b*, which terminates at the frequency ω_{SO}. One of the degenerate modes of branch 2*b* is a convective instability—here the slow SSCW (branch *b*) and the optical phonons (branch 2) interact, producing amplification of the slow SCW, in essentially the same manner as a resistive medium produces slow SCW amplification.[20,14] The optical phonons behave as positive-energy waves, as discussed previously.

In addition to branch 2*b* of Fig. 3, another polariton branch, namely 5, begins at $\omega=\omega_T$ and, with increasing frequency, becomes a coupled plasmon-phonon mode. It then bends upward, becoming parallel to the recovered branch *b*, which moves in from large wave vectors.

In comparing Fig. 1 with Figs. 2 and 3, one notices that the inclusion of retardation—with the resultant addition of two more branches—complicates the branch interactions. Because the branch coupling that results in amplification is of most interest, we will comment on this first. In Fig. 1, the slow SSCW interacts with the optical phonons to produce an amplifying instability. With the introduction of retardation (Fig. 3), the same coupling of the SSCW and optical phonons produces amplification. In addition, however, there are two evanescent branches for the retarded case. The evanescent branch 1*a* of Fig. 2 is similar to that found in the situation without optical phonons for the geometry described in Sec. III A above.[14]

In the region of the convective instability, the wave vector is sufficiently large so that the decay constants given by Eqs. (2.3) and (2.11) are nearly equal to the wave vector k_y. Consequently, the electromagnetic surface waves are very localized near the surface, i.e., their penetration depth is small.

C. Retardation effects with carrier damping

Figures 4 and 5 show dispersion curves for the situation where damping is included and $\omega_p=\omega_T$. The presence of damping makes noticeable changes in branch be-

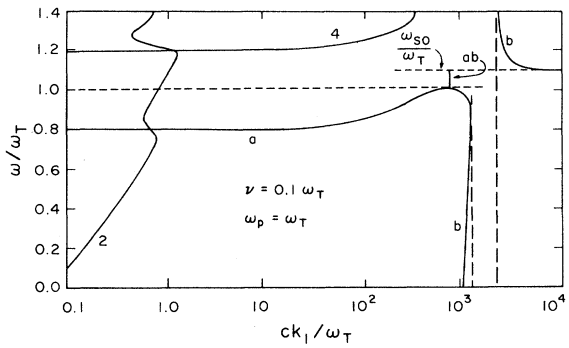

FIG. 5. Retarded dispersion curves with damping for $\omega_p=\omega_T$ and positive wave vector.

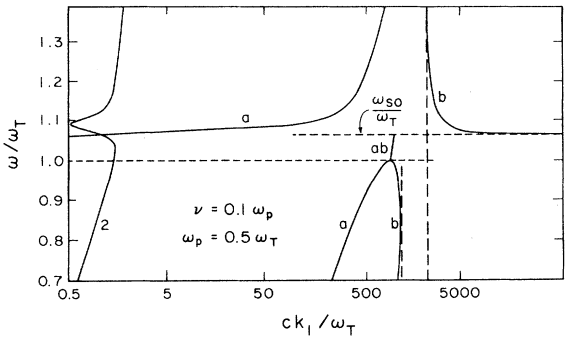

FIG. 6. Retarded dispersion curves with damping for $\omega_p=0.5\omega_T$ and positive wave vector.

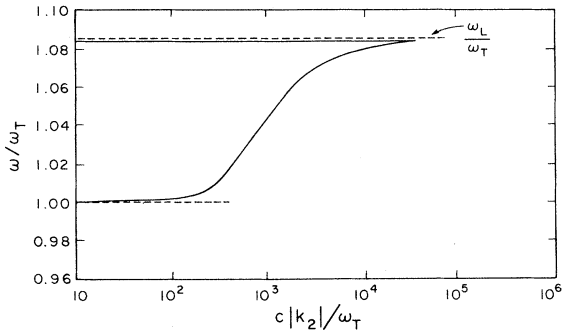

FIG. 8. Frequency dependence of the imaginary part of the wave vector with retardation and damping included for $\omega_p=\omega_T$ and $\nu=0.1\omega_T$.

havior. For example, consider negative wave vectors (Fig. 4). Here branches *a* (fast SSCW) and 1 (polariton) cross, but do not interact to form an instability. Note, however, that in the vicinity of the crossing point, branch 1 does exhibit backbending. In contrast to the situation shown in Fig. 3, branch 2 (polariton branch) in Fig. 5 does not bend over to interact with branch *b* (slow SSCW branch); instead, it is branch *a* (fast SSCW branch) that crosses branches 1 and 2 and joins branch *b* at the point where the degenerate branch *ab* starts. One of the modes of branch *ab* is a convective instability. The degenerate branch (*ab*) terminates at $\omega=\omega_{SO}$, similar to what we have seen in Fig. 3. The behavior of the low SSCW, namely branch *b*, is essentially the same in both Fig. 3 and Fig. 5.

In Figs. 4 and 5 for $\omega\geq\omega_L$, one sees that, for negative wave vectors, branch 4 moves in from large negative wave vectors, crosses branch 1, and proceeds into the regime of positive wave vectors, where it crosses branch 2 and then bends upward in the vicinity of branch *b*. This behavior is to be compared with the same frequency range in Fig. 2. There branch 4 interacts with branch 3 to produce an evanescent wave.

Next we consider the low plasma density case, namely, $\omega_p=0.5\omega_T$. The dispersion curves are shown in Fig. 6. Here the behavior of the branch interactions is qualitatively the same as that shown in Fig. 5, and exhibits an amplifying branch *ab*.

Finally we consider $\omega_p=3.0\omega_T$ (Fig. 7), the high plasma density case. Again there is behavior similar to that of Fig. 3, namely, an amplifying branch *ab*. This is in contrast to the results of Tajima and Ushioda, who found no instabilities for $\omega_p>\omega_T$.

In comparing Figs. 5, 6, and 7, we note that the frequencies associated with the convective or amplifying instability always lie in the range between ω_T and ω_{SO}.

Figure 8 shows the frequency behavior of the imaginary part of the wave vector associated with the amplifying instability of Fig. 5. Similar results for Figs. 6 and 7 are not shown. We see in Fig. 8 that the gain (or loss) begins at $\omega=\omega_T$, and increases with increasing frequency. The gain increases more rapidly as ω approaches ω_{SO}, and then drops to zero.

The results presented thus far show that slow SSCW's interact with optical phonons to produce an amplifying instability. It is therefore of interest to consider the situation where no optical phonons are present. In our previous work[11,12] on silicon in which neither optical phonons nor carrier damping are included, an evanescent mode was found similar to the evanescent mode 1*a* in Fig. 2. We have made calculations in which we include carrier damping but neglect optical phonons. The results are shown in Fig. 9 for negative wave vectors. We see that branch *a*, the fast SCW, crosses branch 1 without interaction, and that branch 1 undergoes backbending as it

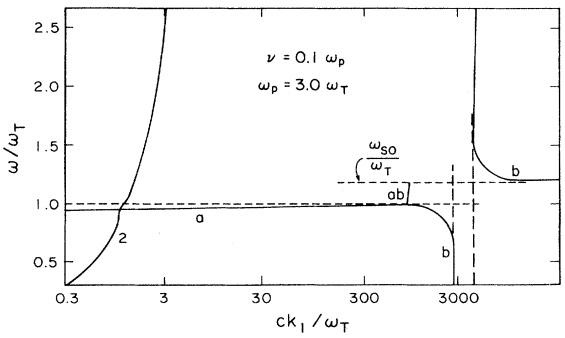

FIG. 7. Retarded dispersion curves with damping for $\omega_p=3.0\omega_T$ and positive wave vector.

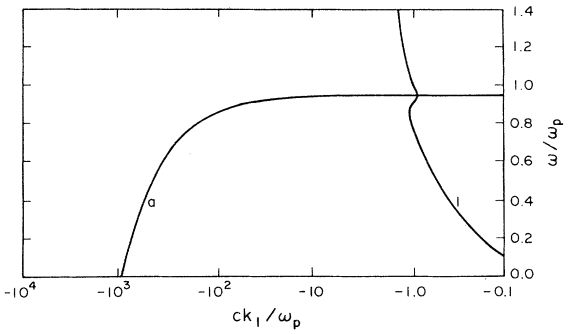

FIG. 9. Dispersion curves including retardation and damping, but without optical phonons, for $\nu=0.1\omega_p$ and negative wave vectors.

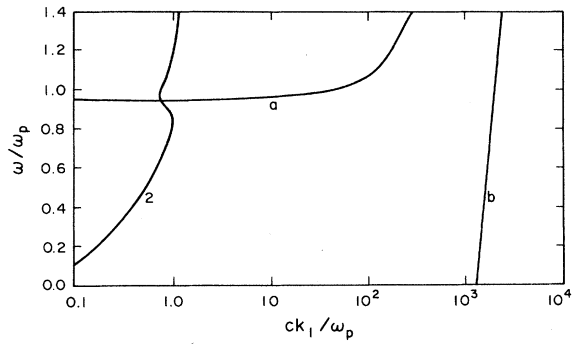

FIG. 10. Dispersion curves including retardation and damping but without optical phonons, for $\nu=0.1\omega_p$ and positive wave vector.

crosses branch *a*. For positive wave vectors, Fig. 10 shows that branch *a* crosses branch 2 without interaction, and that branch 2 undergoes backbending as it crosses branch *a*. Because of the absence of optical phonons, there is no convective instability. In other respects the results presented in Figs. 9 and 10 are quite analogous to those in Figs. 4 and 5, where optical phonons are present. The backbending of the polariton branches near the crossing points with the fast SSCW is a consequence of the damping, as discussed by Kovener *et al.*[21]

In the results presented above, the dispersion relation was solved by taking the frequency ω to be real and then calculating the wave vector k_y which, under certain conditions, turned out to be complex. We have also carried out calculations for the nonretarded case without damping in which the wave vector was taken to be real and the frequency was determined. For a certain range of reduced wave vector $k_y V_0/\omega_T$, a complex-conjugate pair of frequencies results. One mode of the pair corresponds to a convective instability.

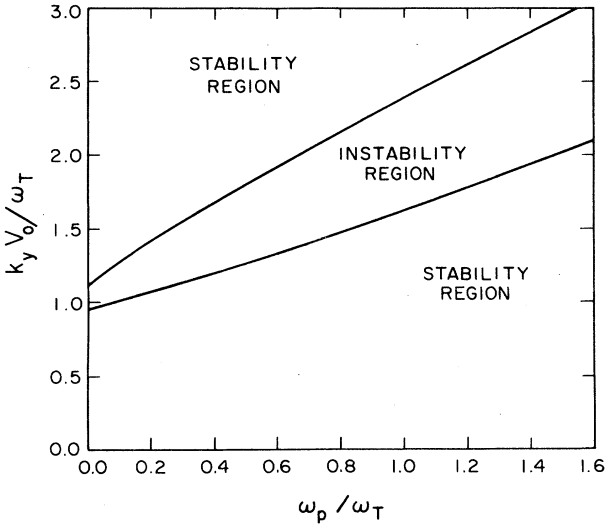

FIG. 11. Wave-vector range for instability as a function of plasma frequency.

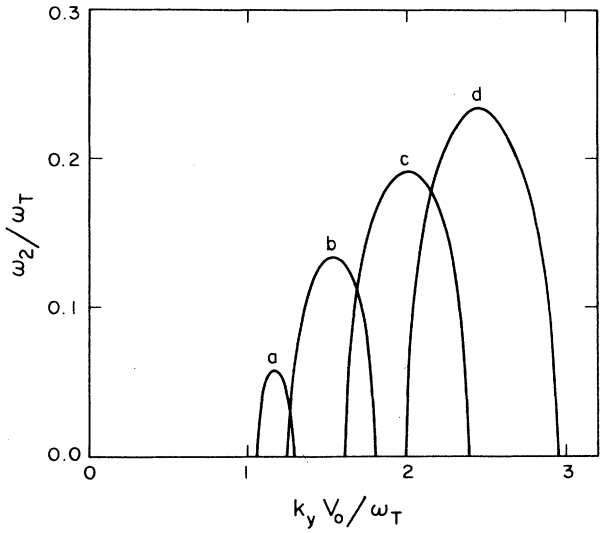

FIG. 12. Imaginary part of the frequency as a function of wave vector for various plasma frequencies: (a) $\omega_p=0.1\omega_T$, (b) $\omega_p=0.5\omega_T$, (c) $\omega_p=\omega_T$, (d) $\omega_p=1.5\omega_T$.

The range of reduced wave vector for which the instability exists is plotted in Fig. 11 as a function of the plasma frequency. We see that both the width of the range and the positions of its boundaries increase with increasing plasma frequency. The value of the magnitude of the imaginary part of the frequency, $|\omega_2|$, is plotted against reduced wave vector in Fig. 12 for various values of the plasma frequency. For the situations presented in Fig. 12 it is evident that the peak value of ω_2 increases with increasing plasma frequency. We also see that the range of wave vector for which an instability exists increases with increasing plasma frequency, in agreement with Fig. 11.

It was mentioned previously that Tajima and Ushioda[15] have considered the problem of optical-phonon interactions in a semiconductor. They obtained dispersion relations both taking into account and neglecting a drift current. To take into account the presence of a drift current in their dispersion relation, they simply replaced ω_p^2/ω^2 by $\omega_p^2/(\omega-kV_0)^2$, where ω_p is the plasma frequency and V_0 is the drift velocity. As can be seen from our formulation, this procedure neglects some of the tensor elements of $\epsilon_{\alpha\beta}$, which are nonzero when a drift current is taken into account. Furthermore, they did not incorporate a condition such as the Kliewer-Fuchs specular-reflection boundary condition into their formulation. Consequently, their dispersion relation differs from ours. In the nonretarded limit, however, the two dispersion relations become the same if the thermal velocity of the electrons is neglected, as has been done by us and by Tajima and Ushioda in their surface-mode calculations.

IV. CONCLUSIONS

Dispersion curves have been calculated for SSCW's interacting with surface-optical phonons in GaAs, both

with and without carrier damping. In both cases an amplifying instability for the slow SSCW begins at ω_T, the transverse-optical-phonon frequency, and terminates at ω_{SO}, the limiting surface-optical-phonon frequency. The slow SSCW acts as a negative-energy wave and couples with the positive-energy optical phonons, thus forming the amplifying instability. This is analogous to the situation where the slow SCW couples with a dissipative medium such as a "resistive wall"[20] or with a stationary plasma.[22]

Since the frequencies associated with the amplifying instability lie between ω_T and ω_{SO}, they therefore correspond to infrared frequencies. By introducing a coupling device such as a grating, it may be possible to exploit the instability to produce a source of infrared radiation.

ACKNOWLEDGMENTS

The work of one of the authors (B.G.M.) was supported by U.S. Army Research Office (ARO) Contract No. DAAL03-86-C-0016 and that of the other author (R.F.W.) by National Science Foundation (NSF) Grant No. DMR-85-17634.

[1]A. Hasegawa, J. Phys. Soc. Jpn. **20**, 1072 (1965).
[2]G. A. Baraff and S. J. Buchsbaum, Phys. Rev. **144**, 255 (1966).
[3]G. S. Kino, Appl. Phys. Lett. **12**, 312 (1968).
[4]M. C. Steele and B. Vural, *Wave Interactions in Solid State Plasmas* (McGraw-Hill, New York, 1969).
[5]Y. Mizushima and T. Sudo, IEEE Trans. Electron Devices **ED-17**, 541 (1970).
[6]T. J. B. Swanenburg, IEEE Trans. Electron **ED-20**, 630 (1973).
[7]N. L. Pandey and R. N. Singh, Phys. Rev. B **14**, 719 (1976).
[8]M. V. Krasheninnikov and A. V. Chaplik, Zh. Eskp. Teor. Fiz. **79**, 555 (1980) [Sov. Phys.—JETP **52**, 279 (1980)].
[9]B. G. Martin, A. A. Maradudin, and R. F. Wallis, Surf. Sci. **91**, 37 (1980).
[10]J. Pozhela, *Plasma and Current Instabilities in Semiconductors* (Pergamon, Oxford, 1981).
[11]B. G. Martin, J. J. Quinn, and R. F. Wallis, Surf. Sci. **105**, 145 (1981).
[12]R. F. Wallis, B. G. Martin, and J. J. Quinn, Surf. Sci. **140**, 64 (1984).
[13]F. Crown, J. Appl. Phys. **57**, 4772 (1985).
[14]B. G. Martin and R. F. Wallis, Phys. Rev. B **32**, 3824 (1985).
[15]T. Tajima and S. Ushioda, Phys. Rev. B **18**, 1892 (1978).
[16]B. G. Martin and R. F. Wallis, Bull. Am. Phys. Soc. **30**, 561 (1985).
[17]B. G. Martin and R. F. Wallis, Bull. Am. Phys. Soc. **31**, 1105 (1986).
[18]B. G. Martin and R. F. Wallis, Bull. Am. Phys. Soc. **32**, 451 (1987).
[19]K. L. Kliewer and R. Fuchs, Phys. Rev. **172**, 608 (1968).
[20]C. K. Birdsall, G. R. Brewer, and A. V. Haeff, Proc. IRE **41**, 865 (1953).
[21]G. S. Kovener, R. W. Alexander, and R. J. Bell, Phys. Rev. B **14**, 1458 (1976).
[22]A. Hasegawa, *Plasma Instabilities and Nonlinear Effects* (Springer-Verlag, Berlin, 1975), p. 17.